SEA ICE TYPE CLASSIFICATION IN BAFFIN BAY AND M'CLINTOCK CHANNEL USING REMOTE SENSING TECHNIQUES

By: Zarrin Tasneem

TA: Aaron Thompson

Date: February 28, 2016

Table of Contents

1 Abstract

Climate change and the loss of sea ice is the biggest threat to Polar Bears due to the destruction of habitat ground and the inability to obtain food. The different sea ice types allow Polar Bears to build dens for habitation and hunt for seals. The change in sea ice type from Baffin Bay and M'Clintock Channel in Nunavut, Canada, will be analyzed. The different types of ice will be classified using the fuzzy support vector machine and the Normalized Difference Snow Index (NDSI) methods. Albedo values for the different ice types will be used to determine what type of ice, the different pixel values fall under. Then the NDSI (Normalized Difference Snow Index) image of the sea ice types will be derived in order to check if the different types of ice are located in the same area for both images produced from the different methods. A majority analysis will be performed on the fuzzy support vector machine to smooth out the image. An accuracy assessment will be carried out on the fuzzy support vector machine to see how accurate the training site selection was. If it wasn't accurate enough, then the fuzzy support vector machine will be performed a few times until the accuracy is above 85%. The two different types of ice which are landfast ice and pack ice will be classified and then the different types of ice such as new ice, young ice, first year ice and then multiyear ice will be classified. Within the young ice stage, there are grey ice and grey-white ice which will also be classified. From these classifications, the Polar Bear vulnerability will be further analyzed. This vulnerability is due to the destruction of the different types of sea ice.

Keywords: Sea Ice Type Modelling, Maximum Likelihood Classification, Majority Filter Analysis

2 Introduction

Loss of sea ice is the biggest threat to the Polar Bear population due to the destruction of their habitat area and the inability to obtain food using their regular procedure. Sea ice allows Polar Bear to build dens for habitation and for seal hunts. In particular, there are two types of ice which are land fast ice and pack ice. Pack ice is ice, which floats on water, whereas landfast ice is attached to the shore and forms along the coast. Within pack ice, there are first year ice, and multiyear ice (National Snow & Ice Data Center). First year ice is ice that melts during the summer melt season period. However, multiyear ice has survived the summer melt period. First year and multiyear ice also have different electromagnetic properties which can be detected by the satellite sensors in order to differentiate between the two types of ice.

There are also other types of ice which vary with thickness such as new ice, and young ice. New ice is less than 10 centimeters thick, young ice is 10 to 30 centimeters thick, first year ice is thicker than 30 centimeters and multiyear ice is 2 to 4 meters thick (National Snow & Ice Data Center). Within, young ice, there are grey ice, which is 10 to 15 centimeters thick and grey-white ice which is 15 to 30 centimeters thick. These types of ice located in Baffin Bay and M'Clintock Channel will be classified and analyzed. First, land fast ice and pack ice will be classified based on the albedo values. Then the first year and multiyear ice

within pack ice will be classified. Next, the remaining types of ice (New ice and young ice) will be classified, if they are prevalent and important for the research.

If young ice is classified, then the two different types of young ice which are grey-ice and grey-white ice will be classified based on the reflectance values to compare the areal difference and how they are affecting the polar bear population.

These sea ices will be classified using the Support Vector Machine and the Normalized Difference Snow Index (NDSI) classification methods. The sea ice types will be classified using the albedo value and then class centers will be determined to reduce outliers. The class centers will also be calculated to make the classifications, more accurate. Training sites will be selected for the different sea ice type and then the SVM and the NDVI will be applied on the image. After running the SVM and NDSI, a majority filter analysis will be used on the SVM classification to smooth out the image. Then the accuracy assessment will be used, from which the confusion matrix will be produced which contains the accuracy value. The accuracy value will determine how accurate the classification was. If the accuracy value produced is above 85% then the accuracy of the classification is really good, otherwise the classification will have to be reproduced.

Hopefully, this project will help to identify the impact of the destruction the different sea ice types on the Polar Bear population to bring awareness about this issue.

4 Sea Ice Type Modelling

4.4 Neighbourhood Supported Classification- SAR

In the article by (Dabbor & Shokr, 2013) for SAR images, neighborhood supported classification was used because the same pixel can have different likelihood assignment for multiple classes. This is for the pixel based approach.. However, two neighboring pixels are not completely statistically independent. If the surrounding pixels around the observed pixel

are classified in a class V_i, it is more likely that the observed pixel belongs to class V_i (Dabbor & Shokr, 2013). The spatial context information is useful for resolving uncertainties in the likelihood assignment values where the vague consistency occurs at small portions. A second spatial-based likelihood assignment value can be calculated for each pixel, based on the surroundings of the observed pixel. Assuming an observed pixel j was classified in one of the M pixels V_1, V_2,..., V_M in the classification iteration of h. An n x n window can be defined in order to estimate the spatial-based likelihood assignment values of the observed pixel to each class by classifying the neighboring pixels in the iteration of h-1. Therefore, the spatial-based likelihood (Support Vector Machine) assignment value Q_s of the pixel j to the class V_i can take the form:

$$Q_{s_{ij}} = \frac{n_i}{n^2 - 1}, \quad i = 1, 2, ...M \qquad (13)$$

(Dabbor & Shokr, 2013)

Where n_i is the number of neighboring pixels which were classified to the class V_i in the classification iteration of h-1 (Dabbor & Shokr, 2013). Instead of iteration of h, iteration h-1 is considered, because the neighboring pixels surrounding the chosen pixels are not assigned to specific classes in the iteration yet. Second, the classification approach is an iterative supervised approach which is conducted from the selected training sample of pixels. If the spatial context information is considered, a total likelihood assignment value called Q_t can be calculated for a pixel j using the equation:

$$Q_{t_{ij}} = Q_{n_{ij}} + \lambda Q_{s_{ij}} \qquad (14)$$

(Dabbor & Shokr, 2013)

Where λ is a weight parameter, which determines the contribution of the spatial based likelihood assignment value on the total likelihood assignment value.

$$Q_{n_{ij}} = \frac{Q_{ij}}{\sum_{i=1}^{M} Q_{ij}}, \text{ where } i = 1,2,\ldots,M \qquad (15)$$

(Dabbor & Shokr, 2013)

Therefore, for SAR images, the total likelihood assignment values can be between 0 and 2, instead of 0 and 1, which is only applicable for MODIS images when applying the fuzzy support vector machine approach. In equation 14 (on page 5), the quantities Qn_{ij} and Qs_{ij} are added together in order to estimate the final membership assignment value of a pixel (Dabbor & Shokr, 2013). The contribution of this information to the classification result depends on the value of the weight parameter, such as λ=1

4.1 Albedo/ Reflectance values of Sea Ice types

Surface albedo is the ratio of solar energy directed upwards from a surface over the incident energy that hits the surface (with snow and/or melt ponds on it) (Fetterer, & Untersteiner, 1998). It is measured in the optical region of the spectrum with wavelengths between 300 and 3000 nm. The formation of ponds and the drop in albedo causes removal of rapid sea ice through an ice-albedo feedback process. Ice-albedo feedback process is a climate process of positive feedback, where a change occurs in the area of snow-covered land, ice caps, glaciers or sea ice. This process alters the albedo. Sea ice albedo is a critical parameter, which controls shortwave responses in the surface energy balance and has been a major focus in several modelling and observational studies. The most responsive region (to changes in the sea ice surface) within this spectrum is the visible and part of the near infrared region. Sea ice surface albedo can be derived from satellite sensors in the visible and

near-infrared wavelengths (Fetterer, & Untersteiner, 1998). This can obtain albedo estimates for climate-scale studies and modelling. According to the article by (Hanesiak et al., 2001), the albedo for bare first year ice is 0.52 and for melting white ice and frozen white ice, the albedo is from 0.56 to 0.68 and 0.7 respectively.

4.3 Fuzzy Support Vector Machine

The theory of support vector machines is based on the idea of landcover error minimization (Lin & Wang, 2002). SVM provides high performance in comparison to traditional learning machines and it's also a powerful tool for solving classification problems. SVM maps the input image into a high dimensional feature space and finds a separating hyperplane that can maximize the margin between two classes in this space (Lin & Wang, 2002). Maximizing the margin is a quadratic problem and can be determined by introducing Lanrangian multipliers. Lanrangian multiplier is a method for finding the local maxima and minima of a function, which contains equality restraints. SVM finds the ideal hyperplane by using the dot product functions on the feature space called kernels. The solution of finding the optimal hyperplane is a combination of a few input pixels, called support vectors (Lin & Wang, 2002). In this study, a fuzzy membership was applied to each input pixel for SVM and it was reconstructed into fuzzy SVM so different input pixels can contribute differently to the decision of the classification process. This enhances the SVM classification process by reducing the effect of outliers and noises in the image.

Suppose we have a set S of labelled training points.

$$(y_1, \mathbf{x}_1), \ldots, (y_l, \mathbf{x}_l). \qquad (1)$$

Each training point $\mathbf{x}_i \in \mathcal{R}^N$ belongs to either of the two classes and is given a label $y_i \in \{-1, 1\}$ for $i = 1, \ldots, l$. The search for a suitable hyperplane in an input feature space is too restrictive. "The solution to this situation is mapping the input space into a higher dimension feature space and looking for the best hyperplane in the feature space. In order to find the hyperplane, the equation below must be used:

$$\mathbf{w} \cdot \mathbf{z} + b = 0 \qquad (2)$$

Defined by the pair (w, b), point x_i can be separated according to the function:

$$f(\mathbf{x}_i) = \text{sign}(\mathbf{w} \cdot \mathbf{z}_i + b) = \begin{cases} 1, & \text{if } y_i = 1 \\ -1, & \text{if } y_i = -1 \end{cases} \qquad (3)$$

Where $\mathbf{w} \in \mathcal{Z}$ and $b \in \mathcal{R}$.

The inequalities below

$$\begin{cases} (\mathbf{w} \cdot \mathbf{z}_i + b) \geq 1, & \text{if } y_i = 1 \\ (\mathbf{w} \cdot \mathbf{z}_i + b) \leq -1, & \text{if } y_i = -1, \end{cases} \quad i = 1, \ldots, l \qquad (4)$$

are applicable for all the elements of the set S. For the linearly separable S, an ideal hyperplane, which is unique, can be determined, where the margin between the training sites for different classes can be maximized (Lin & Wang, 2002). If the set S is not linearly separable, violations in classification has to be allowed in the SVM formulation. For SVM, only a function K, called kernel is required to compute the dot product of the data points in feature space Z that is:

$$\mathbf{z}_i \cdot \mathbf{z}_j = \varphi(\mathbf{x}_i) \cdot \varphi(\mathbf{x}_j) = K(\mathbf{x}_i, \mathbf{x}_j).$$

To construct an SVM classifier, the polynomial kernel of degree d can be used:

$$K(\mathbf{x}_i, \mathbf{x}_j) = (1 + \mathbf{x}_i \cdot \mathbf{x}_j)^d$$

In the training set 1, each training pixel is associated with one class or the other (Batuwita & Palade, 2010). It is required that the important training pixels have to be classified correctly. Each training pixel doesn't belong to one of the two classes. 90% of the training site may belong to one class and 10% may be useless or 20% might belong to one class and 80% might be meaningless. There was a fuzzy membership affiliated with each training pixel. This suggests, the attitude of the corresponding training pixel might flow towards one class or the other in the classification problem (Lin & Wang, 2002). The fuzzy membership is the attitude of the corresponding pixel towards one class and the parameter is a measure of error in the SVM. However, it is a measure of error with different weightings.

The only free parameter, which is C in SVM controls the tradeoff between the maximization of the margin and the amount of misclassifications that take place. A large C makes the training of SVM less misclassified with a narrower margin. The decrease in C would allow SVM to ignore some of the training pixels and set a wider margin (Lin & Wang, 2002). In FSVM, C can be set as an adequately large value, where the system will have a narrower margin which would lead to less misclassifications, if s_i is set to 1 (fuzzy membership=1). A small value for fuzzy membership will cause the corresponding pixel to be less important in the training.

To choose a fuzzy membership, the lower bounds of the fuzzy membership must be defined. Second, the main property of the data set must be selected to connect the land area and the

fuzzy memberships (Lin & Wang, 2002). First $\sigma > 0$ will be selected as the lower bound of the fuzzy membership. Secondly, time will be identified as the main property of this problem, which will make the fuzzy membership s_i, a function of time t_i.

$s_i = f(t_i)$

x_l, the last point should be the most important so $s_l = f(t_l) = 0$ should be chosen and x_1, which is the first point should be the least important, where $s_1 = f(t_1) = \sigma$ should be selected. In order to focus on the accuracy of classifying one class, it must be indicated that 1 represents the pixel that belongs to the class with very high accuracy (Lin & Wang, 2002). If the machine says -1, it belongs to the class with a low accuracy or another class. Different fuzzy memberships can be applied to different classes, where the FSVM finds the best hyperplane with errors appearing only in one class. The FSVM can classify the class, which contains crosses with high accuracy and squares with having low accuracy. Usually, SVM assigns equal weights to all of the pixels so they all have the same importance in determining the margin (Lin & Wang, 2002). However, with the fuzzy support vector machine (FSVM), a weight can be assigned for each training site. Then SVM can be applied to reduce the effects of outliers and noisy pixels. The value of the pixel, which is based on the "truthfulness", is known as the membership value. For each attribute of a class, a membership function can be defined. The membership values for every instance is between [0,1], where 1 shows the absolute truth and 0 shows the absolute false. If the membership values fall within the specified range then the value would be assigned to that class (Lin & Wang, 2002).

The ice type which will be classified in this study, are the first year ice and the multiyear ice, both of these fall under pack ice (National Snow & Ice Data Center). Pack ice is large piece of ice floating in the ocean. Multiyear ice is stiffer and contain more pockets

than first year ice. It is more difficult for ice breakers to clear multiyear ice. Multiyear ice provides the freshwater necessary for polar bear expeditions. There are also new ice, young ice and landfast ice which will also be classified. New ice is known as recently formed. They are composed of ice crystals, which are weakly frozen together and maintain a definite form while they are a float. Young ice is referred to as the ice which is in the transition stage from the thinly formed ice (which is breakable) to first year ice. Fast ice is referred to as the ice which forms and remains attached to the shore (to an icewall) (National Snow & Ice Data Center).

4.2 Use Class Centers to Reduce the Effect of Outliers

A model can be created by setting the fuzzy membership as a function of the distance between the pixel and its class center (Lin & Wang, 2002). If the distance between an outlier and its corresponding mean is equal to the radius, the fuzzy membership would be a function of the mean and the radius of each class. The two points would be regarded as less important in FSVM training sites since there is a huge difference between the hyperplanes found by SVM and FSVM. In contrast, when classifying sea ice types using SAR images, selecting the training sites according to the maximum likelihood rule minimizes the probability of error (Lin & Wang, 2002). For MODIS images, this will be done by using class centers. If assignments made for the M classes in an image are composed of M classes with $N_1,..., N_M$ number of samples (pixels) in each class, then the pairwise Wishart Bayes R_{ij} for classes V_i and V_j can be generalized for the multiclass problem. Eq. (12) can be used with a maximization technique to derive the maximum likelihood polarimetric segmentation technique (Lin & Wang, 2002).

$$\mathbf{z}_i \cdot \mathbf{z}_j = \varphi(\mathbf{x}_i) \cdot \varphi(\mathbf{x}_j) = K(\mathbf{x}_i, \mathbf{x}_j). \qquad (12)$$

(Lin & Wang, 2002)

Equation 10 can be used to construct the best hyperplane, in order to find the class centers for classification (Lin & Wang, 2002).

$$\bar{\mathbf{w}} = \sum_{i=1}^{l} \bar{\alpha}_i y_i \mathbf{z}_i \qquad (10)$$

4.5 Normalized Difference Snow Index

The Normalized Difference Snow Index can be calculated using reflectance values. According to the article by (Xiao, Shen, & Qin, 2010), laboratory-based reflectance measurements was collected for four types of snow/ice cover with different grain. It was found that large reflectance values were present in the visible spectral bands, and very small reflectance values in the mid-infrared band, which was due to snow absorption (Xiao, Shen, & Qin, 2010). The difference in the reflectance values from the visible bands and the mid-infrared bands resulted in large NDSI and NDSII values for snow/ice cover. It was suggested by (Hall et al., 1998) that a NDSI threshold of 0.4 should be used to map snow cover. With a NDSI threshold value of 0.4, it was estimated that the snow/ice area covers approximately 85, 387 pixels in the study area.

According to the article by (Salomonson, 2006), NDSI is a spectral band ratio that considers the fact that snow reflectance is high in the visible wavelengths and low in the shortwave infrared region. This ratio is useful in separating snow from nonsnow-covered surfaces, such as ice. The NDSI is the difference in reflectance values, which are observed in

the visible band such as the MODIS band 4 and a shortwave infrared band such as MODIS band 6, divided by the sum of the reflectance values.

NDSI = (b4-b6)/(b4+b6)

(Salomonson, 2006)

The NDSI was computed using the above equation. The NDSI is computed on a pixel-by-pixel basis. The snow cover area can be determined if the NDSI is greater than 0.4, the reflectance in the near-infrared band is greater than 0.11 and the green band is greater than 0.1. NDSI can also be performed using the sea ice surface temperature to detect the sea ice when the sunlight is not present in the image (Salomonson, 2006). According to the article by (Khalsa, 2002), figures 1 and 2 of the Chukchi sea and Bering Strait show different types of sea ice and the classification of the sea ice types using the NDSI approach. The NDSI and the SVM classification methods will be compared to determine the similarities and the differences between the two types of classification approaches. This process can be useful to further judge the accuracy of the prominent classification approach in the research.

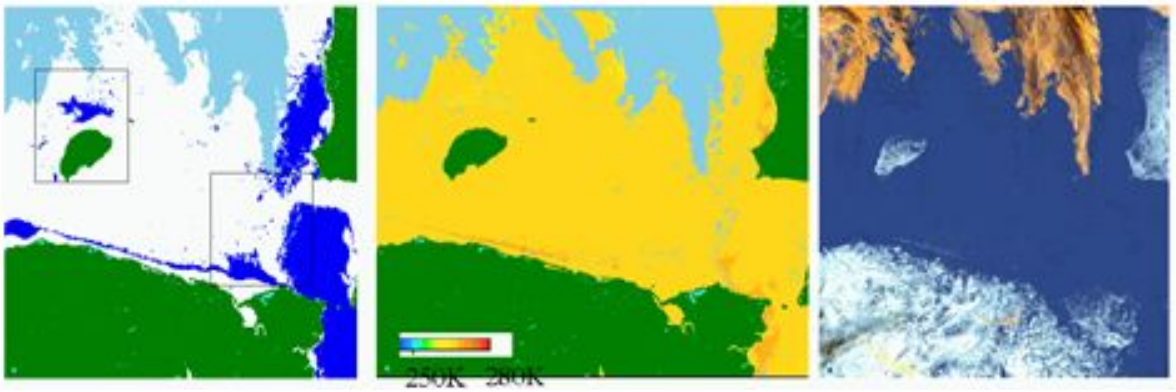

(Khalsa, 2002)

Figure 1

In the figure above, the image on the left displays the MODIS sea ice product produced by the NDSI classification method. The image in the center displays the temperature calculated using the IST method. The image on the right displays the composite image from the MODIS bands 20, 22, and 23.

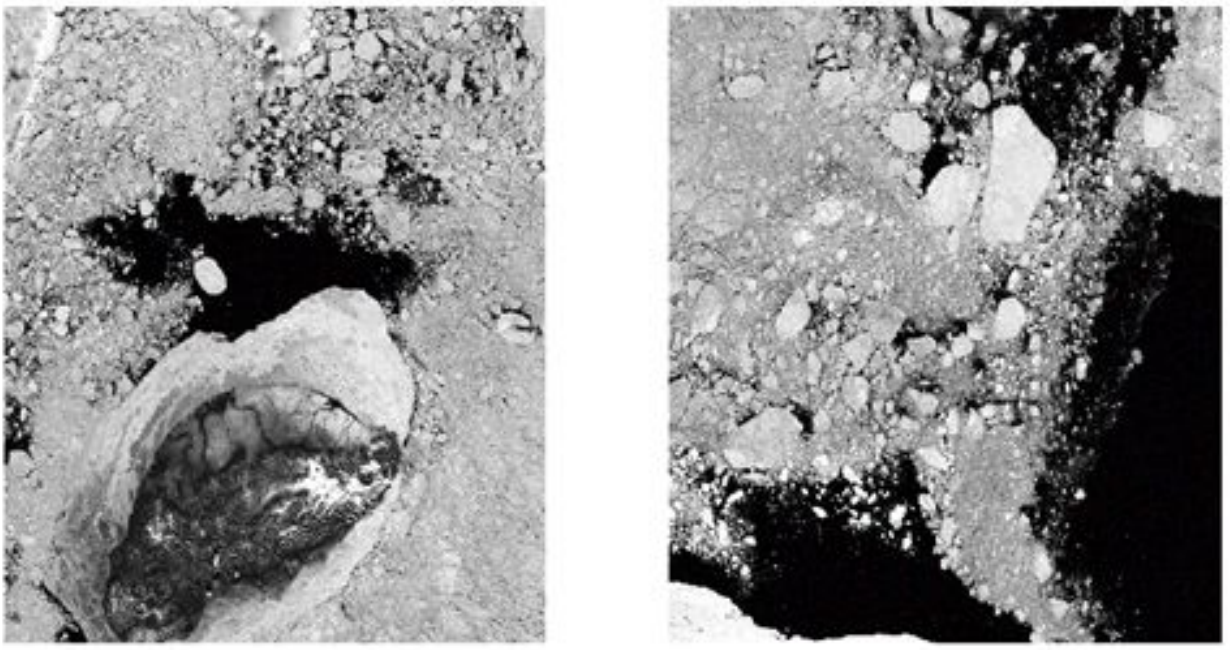

(Khalsa, 2002)

Figure 2

The figure above displays the image coverage of the Chukchi Sea and Bering Strait

4.6 Majority Filter Analysis

A majority filter is defined by specifying a classified image and a threshold value (Kwang, 1996). For each pixel, the number of pixels from each class in the image is considered. If the number, which corresponds to the most common class exceeds the threshold value, the central pixel in the operator window is assigned the most prevalent class. Generally, the most commonly used rule for the majority filter is the five-majority rule, where the kernel size is a 3 x 3 rectangle window and the threshold value is 5 pixels.

Conventional majority filter does not change the land cover type of the central pixel since no majority exists in that type of filtering. In the article by ((Kwang, 1996), the classification confidence of a first decision rule is considered, in order to decide whether the central pixel should be a mixed pixel or not. A mixed pixel can have the spectral signature of a different class than those of the mixing components (composed of different classes). For this study since the SVM was applied as a first decision rule to produce a land cover map, the SVM probability was used as the classification confidence. In other words, the SVM classification image was used for the input (Kwang, 1996). "In order for the central pixel to be regarded as a mixed pixel, the class of the central pixel must have the lowest frequency in an operator window" (Kwang, 1996). The first majority class that is determined by the majority filter is allocated as the central pixel. The allocation of high confidence class among the mixed land cover types in the image may improve the accuracy of the classification (Kwang, 1995).

In the article by (Qian, Zhang & Qiu, 2005), the spatial noise is also reduced by the majority filter analysis. In the image processing technique, if the center pixel class is different from the surrounding pixels then the center pixel class will be replaced by the majority class. For the majority analysis, the classification input file can be selected. Then from the list of classes, the majority filter will be applied on the selected required classes. A kernel size and a center pixel weight will need to be selected and applied to determine how many times, the class of the center pixel will be counted (Qian, Zhang & Qiu, 2005).

4.7 Accuracy Assessment

In the article by (Jain, Goswami & Saraf, 2008), more than 30 ground truth ROIs were selected for each image to make sure, the ROIs were spread throughout the study area to

obtain a higher accuracy for the classification. The accuracy of satellite-based estimation of snow covered areas were compared with the ROI ground truth data. Since the ground-truth data of snow covered areas were not available for the study, an indirect approach was used in the article to estimate snow cover using the temperature lapse rate method. Air temperature data was collected for five ground stations. The maximum and minimum air temperature data of the day before and the day after were added with the data of that date for which satellite images were available. An average air temperature was also calculated. Using this air temperature data and the temperature lapse rate method, the altitude that corresponds to 0 degrees Celsius was computed by (Jain, Goswami & Saraf, 2008). The area above this altitude was considered to be covered with snow. The temperature lapse rate value of 0.65uC/100m was used to estimate snow covered areas. The snow covered areas were estimated for all the dates for which the satellite images were found. The result shows that ground-based estimation of snow covered areas were close to the satellite-based estimation.

In another article by (Parajka, Holko, Kostka, Bloschl, 2012), the accuracy of the MODIS snow cover product was quantitatively discovered by using ground measurements. Snow observations along the transect (a straight line that runs through a feature, along which observations were made or measurements were taken) are considered as ground truth for the pixel, closest to the location of the snow measurements. If the ground "SWE" (Snow Water Equivalent) measurement is bigger than zero, the pixel is considered as snow covered. The information on when the snow melted was not available, so the snow cover mapping accuracy index (SI) was applied. SI is the ratio of the sum of the station days when the snow was correctly mapped to the total of correctly (A) and falsely (B) mapped snow cover by MODIS.

SI = (* 100 (A/(A+B)))

Where A and B represents the amount of cloud-free ground observations for a particular classification category (Parajka, Holko, Kostka, Bloschl, 2012). From the accuracy assessment, a confusion matrix will be produced, which will be used to quantify the accuracy of the training site selection based on the produced values on the confusion matrix report. If the percentage is above 85% then the classification is good, otherwise the classifications will have to be reproduced.

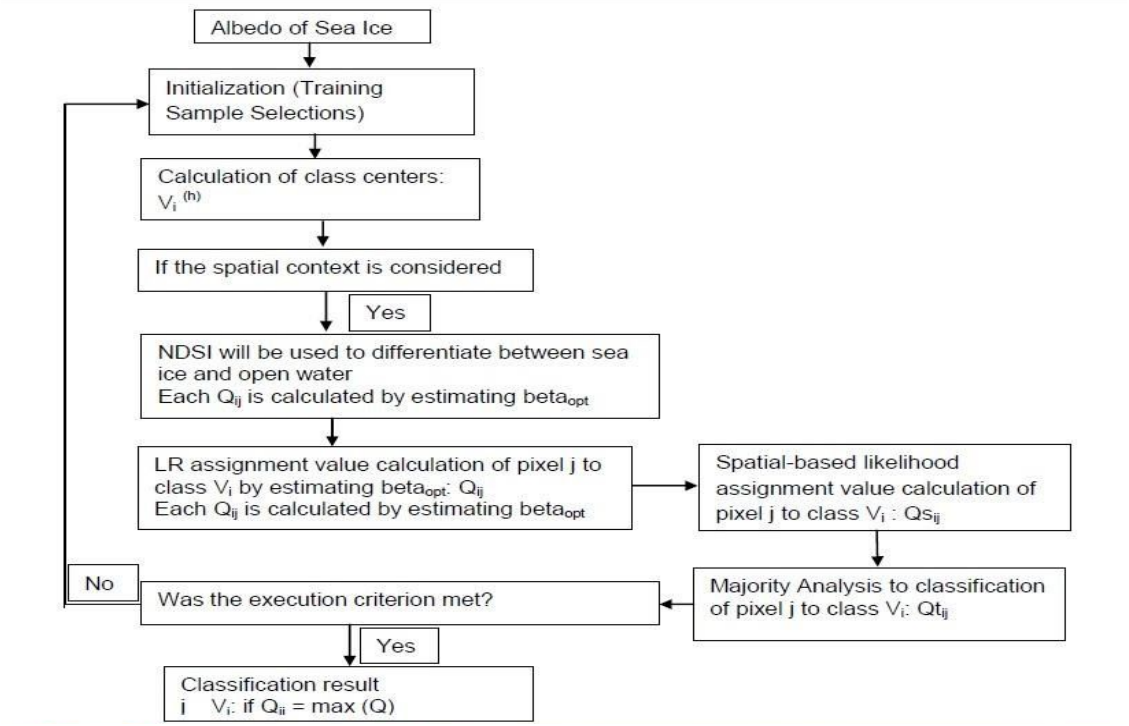

Figure 3

The figure above displays the workflow of the sea ice type classification for MODIS image in conjunction with the sea ice type classification for SAR images.

5 Discussion

5.1 Discussion

The MODIS image was chosen because it is easier to acquire then the other images. It would also be easier to classify the different types of pixels using the MODIS image because

the different types of bands that are located within the MODIS image are useful for better visibility of the different land cover types. SAR image uses the neighborhood supported classification based on the likelihood ratio, to detect the ice types as the visibility of the different ice types within the SAR images aren't as clear. However, since MODIS and SAR images have different properties, the neighborhood supported classification was altered so that it can be implemented on MODIS images, which has never been implemented before as one whole process. One property that is a difference between MODIS and SAR is the difference in types of band for the two types of images. For example, SAR has polarimetric bands (HH, VH, VV, HV), whereas MODIS images have Visible, Thermal infrared and near infrared bands.

The classification approach was changed from the maximum likelihood classification to the support vector machine classification because after reading different articles, it was established that support vector machine, in fact is more reliable and accurate than the maximum likelihood classification, based on the previous course (Geog 371). It was found that the SVM classifies land cover types more accurately according to the training site selection. However, the image isn't as detailed as the ML classification. The majority filter analysis will be applied later in the method to smooth out the image and also to reduce the "salt and pepper effect" left by the SVM classification.

The different sea ice types can be better detected in the MODIS image because they will first be differentiated using the albedo values. This will allow the determination of the location of the ice types in the image, since the ice types are only portrayed as either white or black in the MODIS image. Once the different ice types are classified with different colours using the SVM classification approach, the different ice types will be easier to visualize. This will be useful for the analysis of the impact of the sea ice types on the polar bear population,

in comparison to analyzing an image that displays ice as only white and black, which is difficult to separate with the naked eye. The MODIS image would not be helpful in analyzing the effect of sea ice types on the polar bear population because the different types of sea ice is not visible, as new ice is displayed as white in the image and the older ice as black.

The effect of sea ice types on the polar bear population is an important topic to pursue because the different sea ice types allow different functions for polar bears. For example, pack ice allows polar bears to migrate from one place to another and find food, as polar bears hunt seal. Landfast ice allows polar bears to build shelter and a place walk around, as it is located along the shore.

5.2 Weakness

The different articles that were obtained dealt with different small aspects of the method. However, they did not delve further into the topic, nor did they explore other methods of analysis for the sea ice type analysis. The method for performing the sea ice type classification using the SAR image was also very vague as they did not describe the methods that were required in more detail for the analysis of this topic. Therefore, this method can be rendered time-consuming because extensive research will have to be conducted to determine a suitable approach for the classification of the sea ice types. Another weakness was that their primary focus of research was mathematically modelling each classification approach for the analysis of the sea ice type, instead of how it can be conducted for MODIS images. Plenty of research had to be conducted in order to find relevant articles that outlined sea ice type classifications. There are a lot of articles outlining the sea ice type classification and analysis for SAR images rather than MODIS images.

5.3 Strengths

There were consistencies among the articles about methods for classifying and deriving sea ice types. Along with providing methods to visually display the sea ice type classification, and providing mathematical derivation of the methods, the articles also provide helpful examples on how the sea ice type classification images should look, what they should convey, and how they can affect the environment. The methods can be applied to accurately display the sea ice type classification and to analyze the images. The proposal will provide detailed information related to the study, which can help to make suggestions on reducing the decrease in the sea ice types. The class centers for the pixels will be calculated using the mathematical models that were obtained from the articles, in order to determine the weighting of the different classes of the sea ice types from which the classifications can be derived.

5.4 Limitations/Challenges

The mathematical model to determine the weighting has never been studied so further research will need to be conducted on the mathematical models to understand the models better. Another limitation is that the method is fairly big, which can lead to errors during the processing period. The accuracy assessment can be conducted for the classification but it can't be conducted for the NDSI classification so research will need to be carried out on how to determine if the NDSI classification is accurate. The outputted result will be compared with other NDSI images which were produced for the same topic. Since the training site selection will be conducted manually, it may not be fully accurate so the support vector machine classification will need to be performed a few times. This will be inefficient, along with being time consuming. Comparing the selected training sites with the ground truth ROIs or another input will be difficult, as the ground truth ROIs may not be available online. The

other way of obtaining the confusion matrix will need to be determined through calculations and mathematical modelling if the ground truth ROIs for the sea ice types aren't available.

5.5 Research Gap

This research has never been conducted for a MODIS image, however there is a similar method which has been performed on SAR images. The basics of the method was obtained from the method which was conducted on the SAR images. Even though, there isn't any information for MODIS images, the different parts of the approach has been performed on the MODIS images. Those approaches produce the same output as the approach for SAR images. These approaches were combined into one method and this method only classifies MODIS images to produce the same output as the SAR image for sea ice type classification.

6 Conclusion

Loss of sea ice has a huge impact on the polar bear population. There are different types of sea ice that polar bears use for their survival. These sea ice types are landfast ice and pack ice. Landfast ice is used shelter, whereas polar bears use pack ice for sea hunts. The loss of the different types of sea ice can destroy the polar bear shelters and the foods (such as seals) necessary for their survival. For this reason, it is important to bring awareness about the impact of the loss of the different sea ice types on the polar bear vulnerability. This can be determined by classifying the different sea ice types and then determining the area of the sea ice types. After the different sea ice types are classified and the area of the different sea types are found, the reasons behind the reduction in the different types of sea ice will be discussed. Sea ice types can be classified using the NDSI and the Support Vector Machine classification approaches. For the Support Vector Machine, the albedo and reflectance values would be

determined to determine where the different sea ice are located. Then the class centers to reduce outliers will be calculated and then weighting for the support vector machine will be used to classify the image. Then the majority filter will be used to smooth out the image. Then the accuracy assessment will be carried out to determine how well the SVM was classified and if the classification will need to be reproduced. This can be improved if articles about the different parameter values for classifying sea ice types for MODIS images were available. Then the method for the classification of the different sea ice types could be compared with the articles to better judge if the method is appropriate for this project.

References

1. Batuwita, R., & Palade, V. (2010). FSVM-CIL: Fuzzy Support Vector Machines for Class Imbalance Learning. *IEEE Trans. Fuzzy Syst. IEEE Transactions on Fuzzy Systems, 18*(3), 558-571. Retrieved February 12, 2016, from http://journals1.scholarsportal.info.proxy.lib.uwaterloo.ca/details/10636706/v18i0003/558_ffsvmfcil.xml
2. Canadian Ice Service. (n.d.). Retrieved February 25, 2016, from https://www.ec.gc.ca/glaces-ice/default.asp?lang=En

3. Cheng, M., Chou, J., Roy, A. F., & Wu, Y. (2012). High-performance Concrete Compressive Strength Prediction using Time-Weighted Evolutionary Fuzzy Support Vector Machines Inference Model. *Automation in Construction, 28*, 106-115. Retrieved February 20, 2016, from http://www.sciencedirect.com.proxy.lib.uwaterloo.ca/science/article/pii/S0926580512001331
4. Dabboor, M., & Shokr, M. (2013). A new Likelihood Ratio for supervised classification of fully polarimetric SAR data: An application for sea ice type mapping. *ISPRS Journal of Photogrammetry and Remote Sensing, 84*, 1-11. Retrieved February 25, 2016, from http://journals2.scholarsportal.info.proxy.lib.uwaterloo.ca/details/09242716/v84icomplete/1_anlrfsafsitm.xml
5. Definitions of Lake Ice Terms. (n.d.). Retrieved February 15, 2016, from http://www.geo.mtu.edu/great_lakes/icegroup/ice_terms_jake.html
6. Hanesiak, J. M., Barber, D. G., Abreu, R. A., & Yackel, J. J. (2001). Local and regional albedo observations of arctic first-year sea ice during melt ponding. *J. Geophys. Res. Journal of Geophysical Research: Oceans,106*(C1), 1005-1016. Retrieved February 12, 2016, from http://onlinelibrary.wiley.com.proxy.lib.uwaterloo.ca/doi/10.1029/1999JC000068/abstract
7. Jain, S. K., Goswami, A., & Saraf, A. K. (2008). Accuracy assessment of MODIS, NOAA and IRS data in snow cover mapping under Himalayan conditions. *International Journal of Remote Sensing, 29*(20), 5863-5878. Retrieved February 17, 2016, from http://journals1.scholarsportal.info.proxy.lib.uwaterloo.ca/details/01431161/v29i0020/5863_aaomnascmuhc.xml
8. Qian, Y., Zhang, K., & Qiu, F. (2005). Spatial contextual noise removal for post classification smoothing of remotely sensed images. *Proceedings of the 2005 ACM Symposium on Applied Computing - SAC '05*. Retrieved February 13, 2016.
9. Kim, K. E. (1996). Adaptive majority filtering for contextual classification of remote sensing data. *International Journal of Remote Sensing, 17*(5), 1083-1087. Retrieved February 12, 2016, from http://www.tandfonline.com/doi/abs/10.1080/01431169608949070
10. Kim, K. E. (1996). Adaptive majority filtering for contextual classification of remote sensing data. *International Journal of Remote Sensing, 17*(5), 1083-1087. Retrieved February 13, 2016, from

http://journals2.scholarsportal.info.proxy.lib.uwaterloo.ca/details/01431161/v17i0005/1083_amffccorsd.xml

11. Lin, C., & Wang, S. (2002). Fuzzy support vector machines. *IEEE Trans. Neural Netw. IEEE Transactions on Neural Networks, 13*(2), 464-471. Retrieved February 25, 2016, from http://journals2.scholarsportal.info.proxy.lib.uwaterloo.ca/details/10459227/v13i0002/464_fsvm.xml
12. Mundy, C. J., Ehn, J. K., Barber, D. G., & Michel, C. (2007). Influence of snow cover and algae on the spectral dependence of transmitted irradiance through Arctic landfast first-year sea ice. *J. Geophys. Res. Journal of Geophysical Research, 112*(C3). Retrieved February 13, 2016, from http://primo.tug-libraries.on.ca/primo_library/libweb/action/search.do?fn=search&ct=search&initialSearch=true&mode=Basic&tab=articles&indx=1&dum=true&srt=rank&vid=WATERLOO&frbg=&tb=t&vl(freeText0)=Influence of snow cover and algae on the spectral dependence of transmitted irradiance through Arctic landfast first-year sea ice&scp.scps=primo_central_multiple_fe&vl(631150465UI1)=all_items&vl(1UIStartWith0)=contains&vl(397444794UI0)=any&vl(397444794UI0)=title&vl(397444794UI0)=any
13. National Snow and Ice Data Center. (n.d.). Retrieved February 10, 2016, from https://nsidc.org/cryosphere/seaice/characteristics/multiyear.html
14. Otukei, J., & Blaschke, T. (2010). Land cover change assessment using decision trees, support vector machines and maximum likelihood classification algorithms. *International Journal of Applied Earth Observation and Geoinformation, 12*. Retrieved February 14, 2016, from http://www.sciencedirect.com.proxy.lib.uwaterloo.ca/science/article/pii/S0303243409001135
15. Parandehgheibi, M. (n.d.). Probabilistic Classification using Fuzzy Support Vector Machines. 1-6. Retrieved February 12, 2016, from http://arxiv.org/abs/1304.3345
16. Parajka, J., Holko, L., Kostka, Z., & Blöschl, G. (2012). MODIS snow cover mapping accuracy in a small mountain catchment – comparison between open and forest sites. *Hydrol. Earth Syst. Sci. Hydrology and Earth System Sciences, 16*(7), 2365-2377. Retrieved February 13, 2016.
17. Sakamoto, T., Phung, C. V., Kotera, A., Nguyen, K. D., & Yokozawa, M. (2009). Analysis of rapid expansion of inland aquaculture and triple rice-cropping areas in a

coastal area of the Vietnamese Mekong Delta using MODIS time-series imagery. *Landscape and Urban Planning, 92*(1), 34-46. Retrieved February 14, 2016, from http://www.sciencedirect.com.proxy.lib.uwaterloo.ca/science/article/pii/S016920460900019X

18. Salomonson, V., & Appel, I. (2004). Estimating fractional snow cover from MODIS using the normalized difference snow index. *Remote Sensing of Environment, 89*(3), 351-360. Retrieved February 11, 2016, from http://www.sciencedirect.com.proxy.lib.uwaterloo.ca/science/article/pii/S0034425703002864
19. Salomonson, V., & Appel, I. (2006). Development of the Aqua MODIS NDSI fractional snow cover algorithm and validation results. *IEEE Trans. Geosci. Remote Sensing IEEE Transactions on Geoscience and Remote Sensing, 44*(7), 1747-1756. Retrieved February 17, 2016, from http://journals1.scholarsportal.info.proxy.lib.uwaterloo.ca/openurl?&issn=0196-2892&volume=44&issue=7&eissn=15580644&jTitle=IEEE%20Transactions%20on%20Geoscience%20and%20Remote%20Sensing&aTitle=Development%20of%20the%20Aqua%20MODIS%20NDSI%20fractional%20snow%20cover%20algorithm%20and%20validation%20results&startPage=1747&endPage=1756&year=2006&pubmonth=7&authLast=Salomonson&auinit=V%20V&coden=IGRSD2&doi=10.1109/TGRS.2006.876029&source=primo.exlibrisgroup.com:primo3-Article-ieee&doi=10.1109/TGRS.2006.876029&instance=waterloo
20. Scharfen, G., & Khalsa, S. (n.d.). ASSESSING THE UTILITY OF MODIS FOR MONITORING SNOW AND SEA ICE EXTENT. Retrieved from http://www.eproceedings.org/static/vol02_1/02_1_scharfen1.pdf
21. Threats to polar bears. (n.d.). Retrieved February 14, 2016, from http://wwf.panda.org/what_we_do/where_we_work/arctic/wildlife/polar_bear/threats/
22. Xiao, X., Shen, Z., & Qin, X. (2001). Assessing the potential of VEGETATION sensor data for mapping snow and ice cover: A Normalized Difference Snow and Ice Index. *International Journal of Remote Sensing,22*(13), 2479-2487. Retrieved February 12, 2016, from http://journals1.scholarsportal.info.proxy.lib.uwaterloo.ca/details/01431161/v22i0013/2479_atpovsndsaii.xml